Available online at www.sciencedirect.com
ScienceDirect
Ceramics International 33 (2007) 1419–1425
CERAMICS INTERNATIONAL
www.elsevier.com/locate/ceramint

Synthesis and characterization of calcium aluminate nanoceramics for new applications

M.F. Zawrah *, N.M. Khalil

National Research Center, Ceramics Department, 12622 Dokki, Cairo, Egypt

Received 23 February 2006; received in revised form 7 March 2006; accepted 25 April 2006
Available online 15 September 2006

Abstract

Two types of nanocalcium aluminate powders containing 70 and 60 wt.% Al_2O_3 were prepared by thermal decomposition and investigated in terms of mineralogical composition, hydration, mechanical properties and microstructure. The results revealed that S1 is composed mainly of the CA and CA_2 phases, while S2 composed of CA and $C_{12}A_7$ phases after heat-treatment at 1000 °C. The maximum crystallite sizes for S2 and S1 were 44 and 52 nm and the minimum ones 12 and 19, respectively. Both samples still have small crystallite size after heat-treatment at 1000 °C. The present phases, i.e. CA, CA_2 and $C_{12}A_7$ affect the properties of hydrated and sintered ceramic bodies. S2 hydrated sample achieved higher strength (58.5 MPa) than S1 (52.4 MPa). The higher strength of S2 is ascribed to the presence of CA and $C_{12}A_7$ as a major component, since it reacts rapidly with water. In S1, the poor hydration of CA_2 at the early stage of hydration lowers strength after 7 days hydration as compared with S2. Cold crushing strength (CCS) data of the sintered ceramics bodies exhibit high strength of both samples after firing at 1550 and 1450 °C for S1 and S2, respectively. This is due to the formation of a ceramic bond.

Keywords: Nano-ceramics; Synthesis; Composition; Applications; Properties

1. Introduction

Nanoceramics materials (<100 nm grain size) are in the early stages of development but already show many processing and property advantages over conventional coarse grained alternatives [1]. In recent years there has been increasing interest in the synthesis of nanocrystalline metal oxides [2–5]. It is known that the morphology and particle size distribution are important factors that influence both physical and chemical properties of materials, yet the lack of suitable, consistent, and low cost methods of preparation have limited the ability to control these factors during synthesis.

The term 'high-alumina cement' (HAC) came into use when this type of cement, containing 32–45% Al_2O_3 was introduced in the UK after World war I, to distinguish it from Portland-type cements which contain much less alumina. Subsequently many other aluminous cements have been developed with alumina contents between 50–90%, intended mainly for refractory purposes in the steel industry and as hydraulic material in the cement community [6]. In recent years new applications for calcium aluminates have emerged in optical, bio- and structural ceramics. Some amorphous calcium aluminate compositions are photosensitive and hence are potential candidates for optical information storage devices [7–9]. They also have very desirable infrared (IR) transmission properties for optical fiber application. Crystalline calcium aluminates are used in high-strength and high toughness ceramic–polymer composite materials [10,11]. Conventionally, calcium aluminate cements are obtained by fusing or sintering a mixture of suitable proportions of aluminous and calcareous materials such as CaO or $CaCO_3$ and alumina (Al_2O_3) at temperatures in excess of 1400 °C and grinding the resultant product to a fine powder. Powders produced by this method typically have very low specific surface area (<1 m^2/g) [12,13]. The completion of such reactions depends on the particle size, specific surface area, and the mixing of the reactant powders. Even after repeated firing-grinding cycles to eliminate all of the unreacted materials, the product batch frequently contains undesirable $CaAl_4O_7$, $Ca_{12}Al_{14}O_{33}$ and starting reactants. Uberoi and Risbud [14] and Gulgun et al. [7] synthesized amorphous calcium aluminate powders using chemical processing techniques. The powder produced by the former authors was prepared with aluminum

* Corresponding author. Fax: +202 3370931.
E-mail address: mzawrah@hotmail.com (M.F. Zawrah).

0272-8842/$32.00
doi:10.1016/j.ceramint.2006.04.022

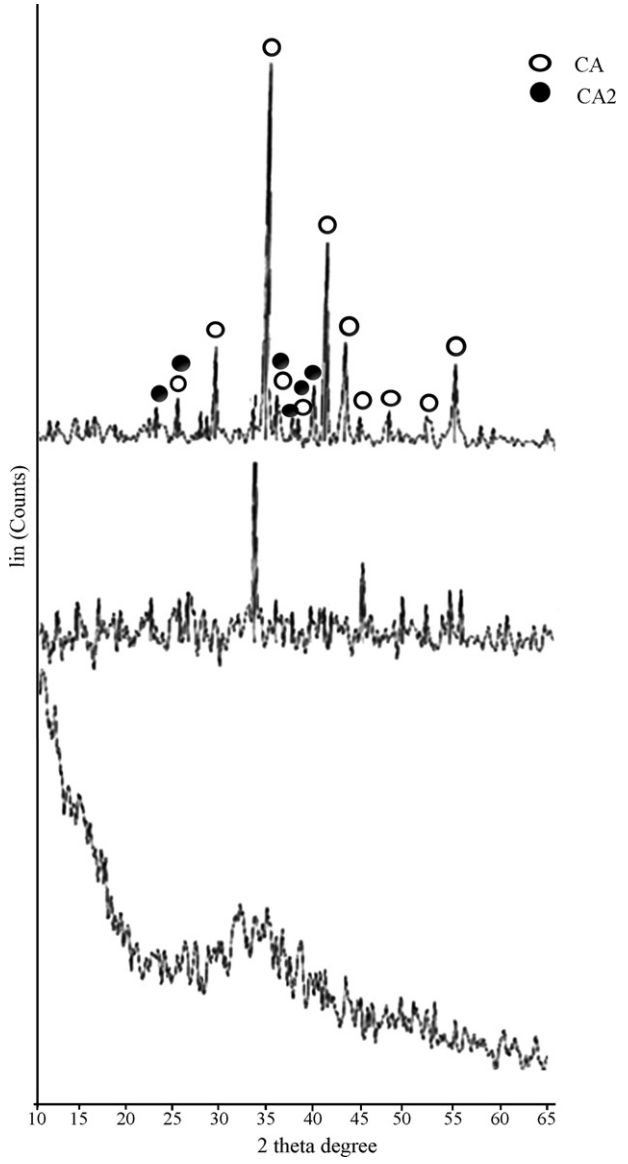

Fig. 1. X-ray diffraction patterns of as prepared (at 500 °C) S1 and calcined at 800 and 1000 °C.

di-sec-butoxide acetoacetic easter chelate [$(Al_9OC_4H_9)_2(-C_6H_9O_3)$] and calcium nitrate [$Ca(NO_3)_2$] precursors in a composition adjusted for $Ca_{12}Al_{14}O_{33}$ synthesis. When calcined below 900 °C, these powders proved to be X-ray amorphous and had a high surface area. Gokats and Weinberg used aluminum sec-butoxide as an aluminum ion source and calcium nitrate tetrahydrate as the calcium ion source. Roy et al. [15] prepared $CaAl_2O_4$ by evaporative decomposition of a solution made from calcium and aluminum nitrate precursors. After a heat-treatment at 900 °C for less than 1 h, crystalline $CaAl_2O_4$ was obtained. The present work aims at the preparation, characterization and sintering of nanocalcium aluminate powders obtained by thermal decomposition.

2. Experimental

Hydrated aluminum nitrate $Al(NO_3)_3{\cdot}9H_2O$ and hydrated calcium nitrate $Ca(NO_3)_2{\cdot}4H_2O$ were weighed and mixed on a laboratory scale to give calcium aluminate containing 70 or 60 wt.% Al_2O_3, which is denoted as S1 and S2 samples. The mixtures were heated in a porcelain dish on a hot plate at about 250 °C until they melted completely, then they were air quenched. The resulting solids were heated at 500 °C for 2 h in electric muffle furnace to complete the thermal decomposition process. After soaking, the powders were quenched and stored in a desiccator. The obtained calcium aluminate powders were calcined at 800 and 1000 °C in a platinum dish using an electric muffle furnace to study the effect of calcination temperature on phase formation. The phase compositions of the co-melted and fired calcium aluminate ceramics were qualitatively determined by XRD using a Philips PW 1710 diffractometer with Cu Kα or Co Kα radiation. To study the grain size, the mean crystallite size was determined from X-ray diffraction broadening and evaluated using the Scherrer formula [16,17]. The morphology of the co-melted powders calcined at 1000 °C was characterized using a transmission electron microscope (Zeiss type EM10).

The obtained calcium aluminate powders were first calcined at 1200 °C, then mixed for 3 min at 25 °C with an adequate amount of water, which was determined for each batch according to the standard ''good ball in hand'' test [18] and cast into cubes in steel mould with dimensions of 1 cm × 1 cm × 1 cm using a vibrating table at a frequency of 50 Hz and 4 min vibrating time. The hydrated cubes were left in their moulds for 24 h in a 100% relative humidity cabinet. The hydrated samples were then demoulded and further cured for 7 days under water in the same cabinet. The hydrated samples were subsequently tested for cold crushing strength (CCS), bulk density (BD) and apparent porosity (AP).

Calcined calcium aluminate powders (at 1000 °C) were semi-dry pressed uniaxially at 60 MPa. The pressed pellets were heated at a rate of 10 °C min^{-1} in an electrical muffle furnace between 1350 and 1550 °C. Densification parameters of the fired samples were determined by means of bulk density,

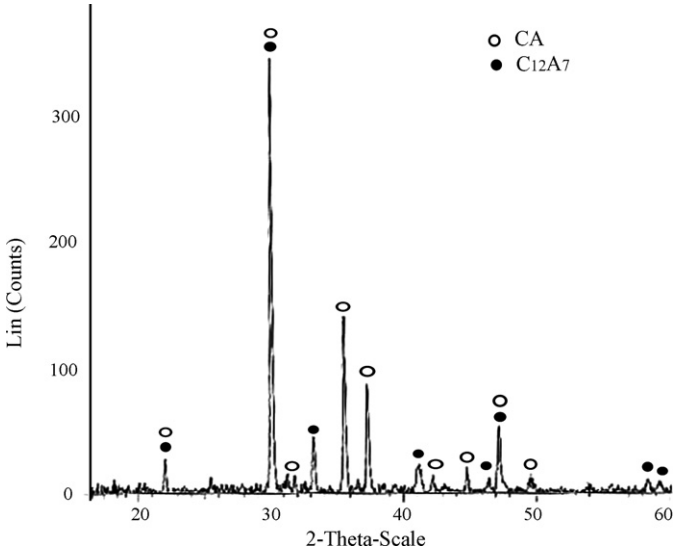

Fig. 2. X-ray diffraction patterns of S2 calcined at 1000 °C.

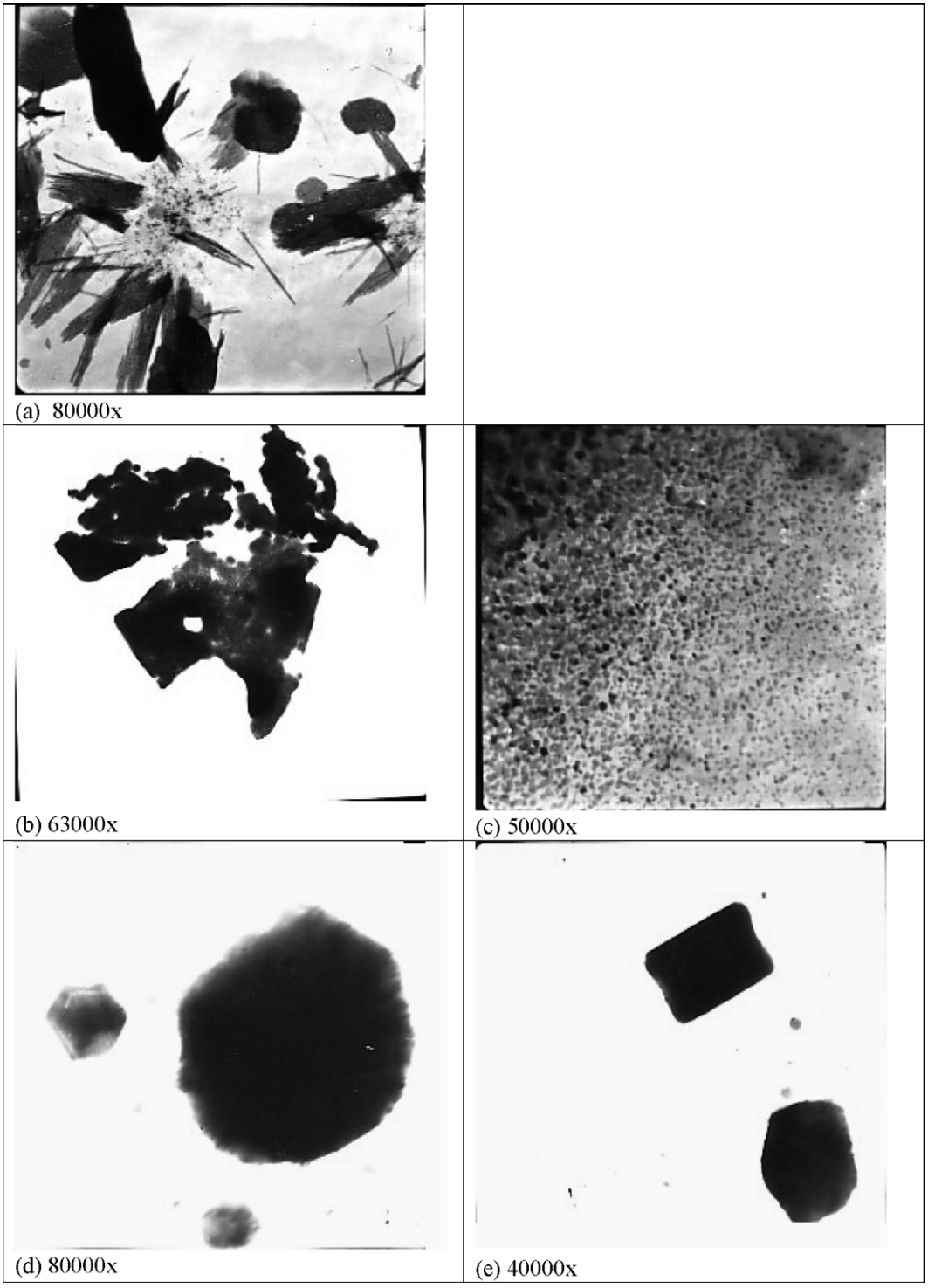

Fig. 3. TEM micrograph of the as prepared (at 500 °C) S1 (a) and those calcined at 800 °C [b (S1) and c (S2)] and 1000 °C [d (S1) and e (S2)].

and apparent porosity according to the Egyptian standard No. 1859- (1990). Microstructure of hydrated and dense samples was investigated using a computerized SEM of the type JEOL, 840.

The mechanical properties in terms of cold crushing strength of the hydrated and sintered calcium aluminate at room temperature were tested.

3. Results and discussion

3.1. Phase composition

X-ray diffraction patterns of as prepared (at 500 °C) calcium aluminate sample S1 and those calcined at 800 and 1000 °C are shown in Fig. 1. On the other hand, Fig. 2 exhibits XRD of S2

sample calcined at 1000 °C. It is indicated from Fig. 1 that the as prepared sample is X-ray pseudo-amorphous pattern, where initial formation of calcium aluminate phases may be envisaged. At 800 °C the sample exhibits some peaks characterizing mono calcium aluminate (CA) and dicalcium aluminate (CA_2). S1 sample calcined at 1000 °C (Fig. 1) is mainly composed of well crystallized mono calcium aluminate and dicalcium aluminate phases. XRD of S2 sample (Fig. 2) shows that the sample is composed mainly of CA with few amount of dodecacalcium heptaaluminate $12CaO{\cdot}7Al_2O_3$ ($C_{12}A_7$).

$Ca_3Al_2O_6$ (C_3A), $CaAl_2O_4$ (CA), $CaAl_4O_7$ (CA_2), and $CaAl_{12}O_{19}$ (CA_6) are the readily formed and thermodynamically stable compounds in the $CaO–Al_2O_3$ binary system with increasing refractoriness in the above order [19,20]. In the conventional preparation route by high-temperature solid-state synthesis, the batch usually contains CaO-rich phases and unreacted Al_2O_3 before the appearance of desired product phase. For example, when a 1:1 mixture of CaO and Al_2O_3 was heated to the temperature range 1200–1400 °C, all of thermodynamically stable phases, i.e. $Ca_3Al_2O_6$, $Ca_{12}Al_{14}O_{33}$, $CaAl_2O_4$, $CaAl_4O_7$, and $CaAl_{12}O_{19}$ were initially formed [21,22]. A single-phase mono calcium aluminate was produced only after a prolonged reaction time at high temperatures in a batch that was proportioned for CA. The formation sequence of phases in these mixtures was always from calcia-rich phases to the proportioned phase. For example, when the starting mix was prepared for CA_2 ($CaO:Al_2O_3 = 1:2$), initially Ca formed in large amounts which, with time and temperature, converted to CA [23]. Singh et al. [21] explained this behavior by a higher reactivity of CaO with respect to Al_2O_3. Contrary to this observation, CA and CA_2 were both observed at early stages of crystallization in chemically prepared mono calcium aluminate powders.

Fig. 3a shows TEM micrograph of the as prepared (at 500 °C) calcium aluminate sample (S1). It appears that the sample exhibits some fiber morphology with some agglomerated particles. Their particle sizes ranged from 10 to 150 nm. S2 sample morphology was the same as S1. On the other hand, TEM micrograph of the same samples calcined at 800 and 1000 °C are shown at two magnifications in Fig. 3b–e. These co-melted powders showed slightly different morphologies with slightly different particle sizes. At 800 °C, agglomerated

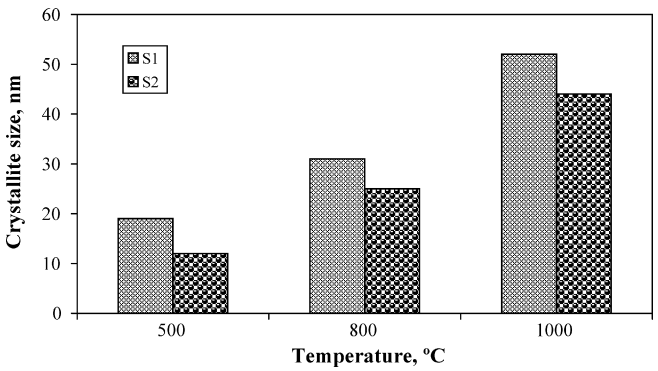

Fig. 4. Crystallite sizes of as prepared S1 and S2 and those calcined at 800 and 1000 °C.

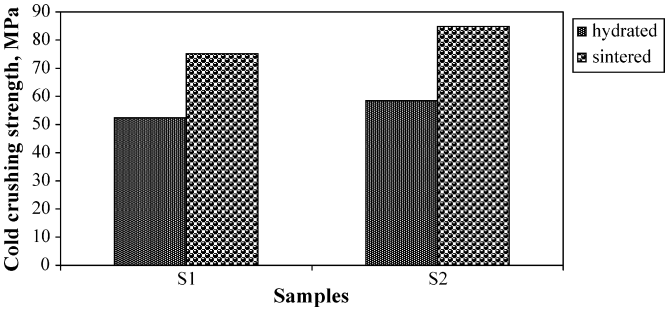

Fig. 5. Cold crushing strength of hydrated calcium aluminate and those sintered at 1550 °C (S1) and 1450 °C (S2).

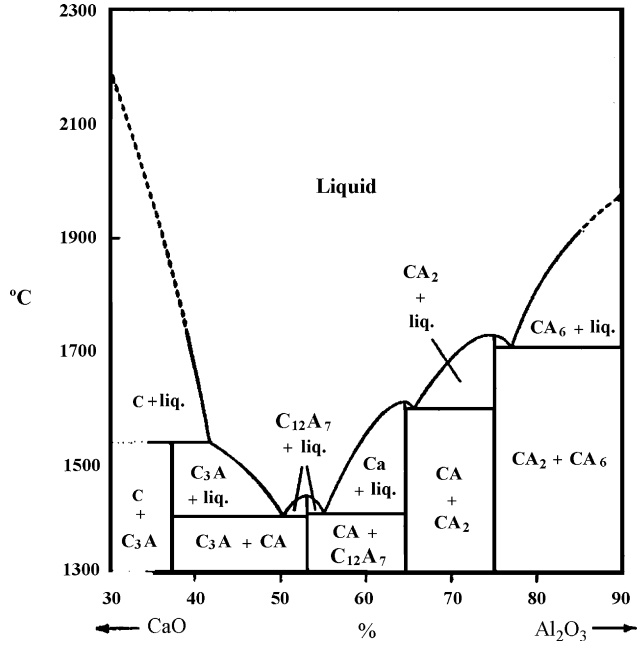

Fig. 6. Phase diagram of $CaO–Al_2O_3$ system.

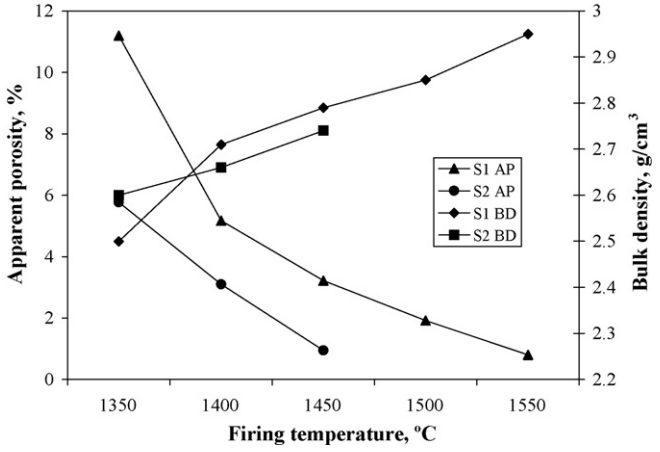

Fig. 7. Bulk density and apparent porosity of the sintered ceramic bodies.

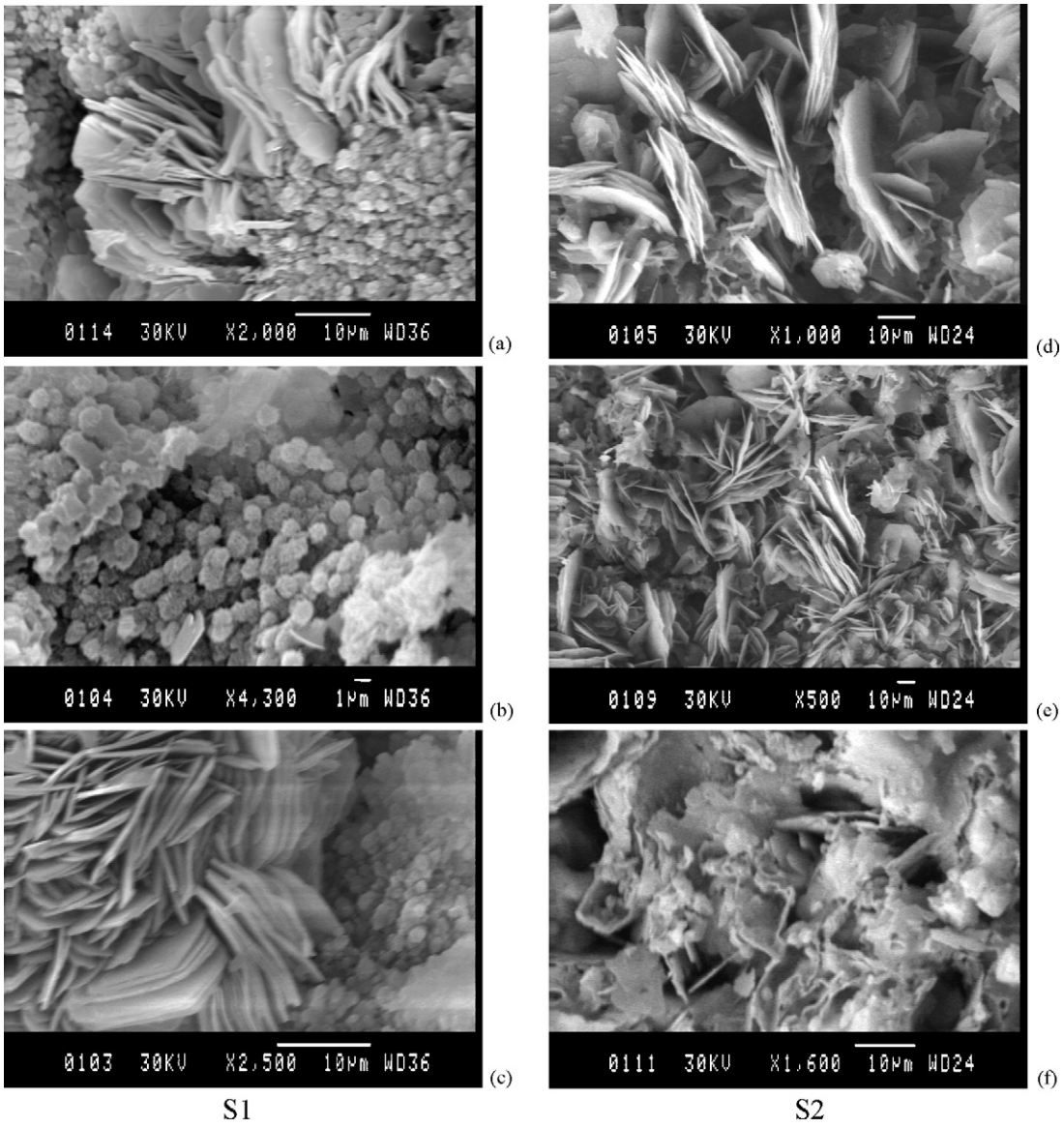

Fig. 8. Photomicrographs of 7 days hydrated S1 and S2.

and spherical cluster morphology of S1 sample with particle size of 20 nm are appeared, but sample S2 exhibits very fine particles with size 10–20 nm. At 1000 °C, well crystalline particles are appeared, i.e. hexagonal shape of S1 sample and monoclinic for S2 sample with particle size ranged between 100 and 150 nm, beside some agglomerated particles. This result is very important because it shows nano-crystalline calcium aluminate ceramics which usually prepared by advanced techniques, can successfully be prepared by the co-melt method using low cost chemicals.

3.2. Crystallite size

Fig. 4 shows effect of heat-treatment at different firing temperature on the crystallite size of the prepared calcium aluminate ceramics. Generally, the crystallite size increases with increasing firing temperature and S1 exhibits higher crystallite size than S2. The maximum crystallite sizes for S2 and S1 are 44 and 52 nm and the minimum ones are 12 and 19, respectively. Both samples still have small crystallite size after heat-treatment at 1000 °C.

3.3. Mechanical properties of hydrated and sintered ceramic bodies

Fig. 5 shows the cold crushing strength of hydrated calcium aluminate for 7 days and those sintered at 1550 °C (S1) and 1450 °C (S2). S2 hydrated sample achieved higher strength (58.5 MPa) than S1 (52.4 MPa). The higher strength of S2 is ascribed to the presence of CA and $C_{12}A_7$ as a major component, since it reacts rapidly with water. It is well known that CA and $C_{12}A_7$ react significantly at early ages of hydration and the hydration of $C_{12}A_7$ is very exothermic so the formation of stable hydrates generally occurs sooner [6]. So S1 gained higher strength at early stages of hydration as compared with S1 which contains CA and CA_2 as a major phase. Although CA_2 is known

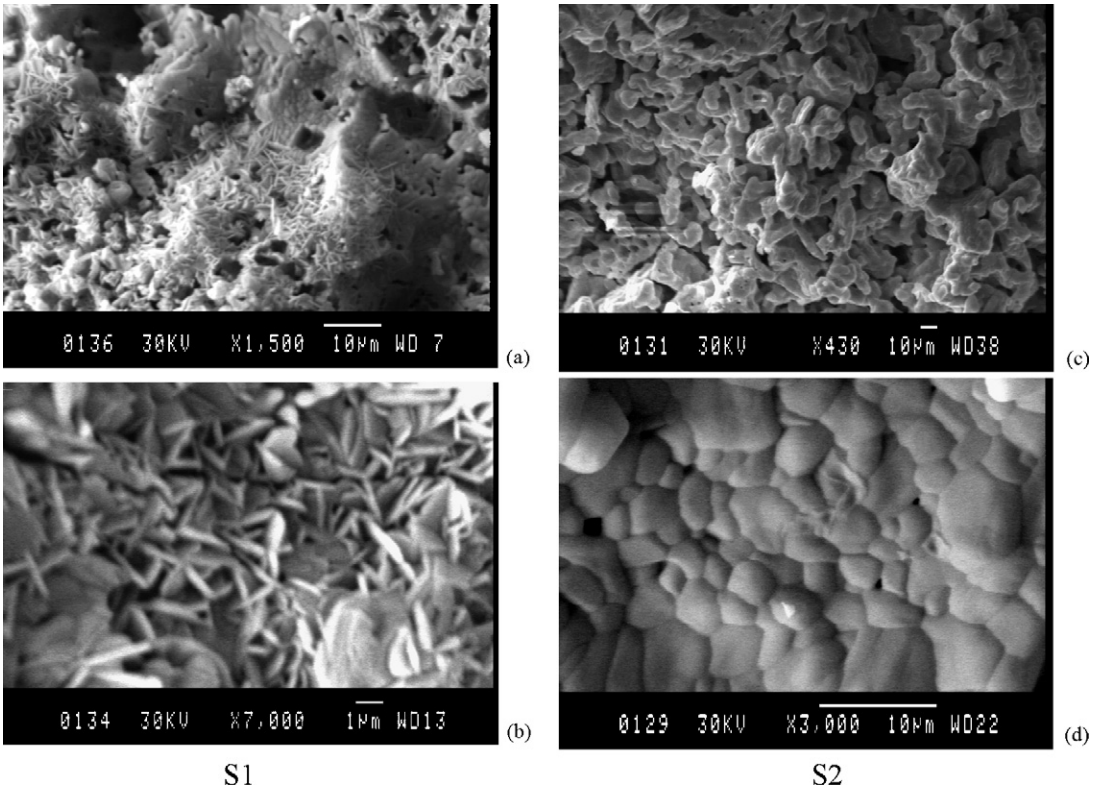

Fig. 9. Photomicrographs of sintered S1 (1550 °C) and S2 (1450 °C).

to react slowly with water in the early stages of hydration, its presence along with CA results in an overall faster hydration rate as the heat of hydration resulting from the hydration of CA activates CA_2 and makes it react relatively faster with water than it would do alone but not than $C_{12}A_7$ [24]. So sample S1 gives lower strength after 7 days hydration as compared with S2 due to the poor hydration of CA_2 at the early hydration stage.

CCS data of the sintered ceramics bodies exhibit high strength of both samples after firing. This is due to the formation of ceramic bond. The higher strength of S2 sintered at 1450 °C is due to the presence of $C_{12}A_7$ which has low melting eutectic point as shown in the phase diagram of CaO–Al_2O_3 (Fig. 6). This low melting phase led to porosity decrease and increase of the mechanical properties.

Fig. 7 shows the bulk density and apparent porosity of the sintered ceramic bodies after firing at different temperatures. The bulk density of S1 increases with increasing the firing temperature reaching its maximum at 1550 °C (2.95 g/cm^3). The bulk density of S2 reaches its maximum value at 1450 °C (2.74 g/cm^3) after which the sample melted. The lower sintering temperature of S2 (at 1450 °C) is due to the formation of a low melting $C_{12}A_7$ phase which helps sintering. The apparent porosity goes oppositely in both samples reaching its minimum value at 1550 °C for S1 (0.80%) and at 1450 °C for S2 (0.95%).

3.4. Microstructure of hydrated and sintered bodies

Fig. 8 shows SEM micrographs of 7 days hydrated S1 and S2 bodies at different locations and magnifications. Networks of well crystallized interlocking hexagonal plates of CAH_{10} and C_2AH_8 could be observed in both samples. These phases are known to be the main hydration product of CA, CA_2 and $C_{12}A_7$ and they play the bonding role in such materials. The higher C/A ratio of $C_{12}A_7$ favors the formation of C_2AH_8 and very little CAH_{10}. Alumina gel (AH_3) was generally observed as structureless grain forming the matrix of this microstructure.

SEM micrographs of the fracture surfaces of the sintered S1 and S2 samples are shown in Fig. 9. It is well known that the structure of calcium aluminate clinker is not easy to identify because there is much more variability from one clinker to another, or even between different parts of the same clinker [6]. Due to the different cooling rates, the crystallite size may vary considerably from fine to coarse. Consequently, different microstructures were obtained for both samples with different grain sizes. S1 exhibits needle-like grains about 200–300 nm in width and about 1.5 μm length interlocked together with the presence of rounded or structureless grains. On the other hand, S2 shows well defined edges grains of about 2–8 μm.

4. Conclusions

It is concluded that S1 is composed mainly of CA and CA_2, while S2 composed of CA and $C_{12}A_7$ phases after heat-treatment. The maximum crystallite sizes for S2 and S1 were 44 and 52 nm and the minimum ones 12 and 19, respectively. Both samples still have small crystallite size after heat-treatment at 1000 °C. The phases present, i.e. CA, CA_2 and $C_{12}A_7$ affect the properties of hydrated and sintered ceramic bodies. S2 hydrated sample achieved higher strength (58.5 MPa) than S1 (52.4 MPa). The

higher strength of S2 is ascribed to the presence of CA and $C_{12}A_7$ as a major component, since it reacts rapidly with water. In S1, the poor hydration of CA_2 at the early stage of hydration lowers strength after 7 days hydration as compared with S2. CCS data of the sintered ceramic bodies exhibit high strength of both samples after firing at 1550 and 1450 °C for S1 and S2, respectively. This is due to the formation of a ceramic bond.

As mentioned before, the obtained amorphous CA can be applied for optical information storage devices, while the crystalline one can be used as structural and bioceramics.

References

[1] M.F. Zawrah, A.A. El-Kheshen, Br. Ceram. Trans. 101 (2) (2002) 71–74.
[2] L.L. Shaw, Z.-G. Yang, R.-M. Ren, Mater. Sci. Eng. A 244 (1998) 113–126.
[3] R.N. Das, A. Pathak, P. Pramanik, J. Am. Ceram. Soc. 81 (1998) 3357–3360.
[4] K. Sureh, K.C. Patil, J. Solid. State Chem. 99 (1992) 12–17.
[5] A.K. Adak, P. Pramanik, J. Mater. Sci. Lett. 17 (1998) 556–559.
[6] F.M. Lea, in: Peter C. Hewlett (Ed.), Lea's Chemistry of Cement and Concrete, Fourth ed., Arnold, 1998.
[7] M.A. Gulgun, O.O. Popoola, W.M. Kriven, Chemical synthesis and characterization of calcium aluminate powders, J. Am. Ceram. Soc. 77 (2) (1994) 531–539.
[8] A.A. Goktas, M.C. Weinberg, Preparation and crystallization of sol–gel calcia–alumina compositions, J. Am. Ceram. Soc. 74 (5) (1991) 1066–1070.
[9] F.T. Wallenberger, N.E. Weston, S.D. Brown, Melt processed calcium aluminate fibers: structural and optical properties, in: Proceedings of the Society of Photo-Optical Instrumentation Engineers, vol. 1484, Growth and Characterization of Materials for Infrared Detctors, SPIE—The International Society for Optical Engineering, Bellingham, WA, 1991 , pp. 116–124.
[10] J.D. Birchall, A.J. Howard, K. Kendall, Flexural strength and porosity of cements, Nature (Lond.) 289 (1981) 388–389.
[11] K. Kendall, J.D. Birchall, A.J. Howard, The relation between porosity, microstructure and strength, and the approach to advanced cement-based materials, Philos. Trans. R. Soc. A310 (1983) 139–150.
[12] K. Fujji, W. Kondo, H. Ueno, Kinetics of hydration of monocalcium aluminate, J. Am. Ceram. Soc. 69 (4) (1986) 361–364.
[13] R.N. Edmonds, A.J. Majumdar, The hydration of mono calcium aluminate at different temperatures, Cem. Concr. Res. 18 (1988) 311–320.
[14] M. Uberoi, S.H. Risbud, Processing of amorphous calcium aluminate powders at <900 °C, J. Am. Ceram. Soc. 73 (56) (1990) 1768–1770.
[15] D.M. Roy, R.R. Neurgaonkar, T.P. O'Holleran, R. Roy, Preparation of fine powders by evaporative decomposition of solutions, Am. Ceram. Soc. Bull. 56 (11) (1977) 1023–1024.
[16] L.L. Shaw, Z.-G. Yang, R.-M. Ren, Mater. Sci. Eng. A 244 (1998) 113–126.
[17] H.P. Klug, L.E. Alexander, X-Ray Diffraction Procedures for Polycrystalline and Amorphous Materials, Wiley, London, 1954, pp. 491–494.
[18] R.E. Fisher, in: Proceedings of 28th Annual Symposium on Refractories, American Ceramic Society, Columbus, OH, 1992.
[19] R.W. Nurse, J.H. Welch, A.J. Majumdar, System $CaO–Al_2O_3$ in a moist-free atmosphere, Fig. 4308, in: M.K. Reser (Ed.), Phase Diagrams for Ceramists 1975 Supplement, American Ceramic Society, Columbus, OH, 1975, p. 103.
[20] O. Kubaschewski, The thermodynamic properties of duble oxides (a review), High Temp.-High Pressures 4 (1) (1972) 1–12.
[21] V.K. Singh, M.M. Ali, U.K. Mandal, Formation kinetics of calcium aluminates, J. Am. Ceram. Soc. 73 (4) (1990) 872–876.
[22] V.K. Singh, M.M. Ali, Formation kinetics of high alumina cements phases, J. Br. Ceram. Soc. 79 (1980) 112–114.
[23] V.K. Singh, U.K. Mandal, Kinetics study of the thermal synthesis of calcium aluminate above 1400 °C, Trans. J. Br. Ceram. Soc. 81 (4) (1982) 112–113.
[24] M.F. Zawrah, N.M. Khalil, Utilization of Egyptian industrial waste materials in manufacture of refractory cement, Br. Ceram. Trans. 101 (5) (2002).